[1]Nyemeesha V

[2]M Kavitha

SCDC-Net: Detection and Classification of Skin Cancer using Deep q Neural Network with Hybrid Features

Abstract: The increment in radiation in atmosphere causing wide spread of skin cancer disease around the globe. Cancer of the skin is one of the most lethal forms of the illness, and it is responsible for millions of deaths annually all over the world. Because of this, the early identification of skin cancer using computer-aided diagnostic (CAD) technology might potentially save a person's life. However, skin cancer classification of performance is affected by hair artifacts and improper segmentation of lesion. The conventional methods were failed to achieve higher performance due to improper feature analysis. Therefore, to achieve the robust performance, this work was developed the transfer learning-based skin cancer detection and classification (SCDC-Net). Initially, UG-Net model was introduced to eliminate hair from skin lesions by enhancing the region of interest, which is developed by combining U-shaped deep learning network (U-Net) with generative adversarial networks (GAN). In addition, Hybrid U-Net (HU-Net) perform the segmentation operation for identifying the disease effected region of interest. Further, the features are extracted using gray level cooccurrence matrix (GLCM) matrix and discrete wavelet transform (DWT), which extracts the color, texture, statistical features. Finally, these combined characteristics are used to train a deep q neural network (DQNN) model, which then classifies a number of different skin cancer illness categories. The simulations conducted on real-time ISIC-2019 dataset proved that proposed SCDC-Net outperformed in all performance measures as compared to existing methods.

Keywords: Skin cancer, computer-aided diagnostic system, generative adversarial networks, U-shaped deep learning network, spatially gray level dependency, deep q neural network.

I.INTRODUCTION

The American Cancer Society has a prediction that there would be around 100,350 cases of melanoma in United States in the year 2020. There is a variety of melanomas diagnosed, of which there will be 60,190 cases in males and 40,160 cases in women. It is estimated that around 6,850 individuals will pass away as a result of melanoma. Based on the differences in age, the percentage of melanomas that have been diagnosed during the last several decades have been rapidly increasing. It is possible to lessen the amount of suffering and loss of life caused by skin cancer by teaching people, especially parents, about the early symptoms and warning signs of the disease. This is the most effective method for reducing the number of individuals who get skin cancer. Melanoma is a very dangerous kind of skin cancer [1]. There are several possible risk factors, including but not limited to: exposure to ultraviolet radiation from the sun, viral infections, exposure to arsenic, immune systems that are already compromised, and some inherited disorders. In the beginning, the only treatment option for melanoma was surgery. As time progressed, however, various methods of treating cancer became available [2]. Surgery remained the only treatment option for melanoma. In today's technologically advanced a civilization, it is considered morally reprehensible to treat or minimize the severity of cancer using traditional procedures or approaches. Because of the rapid advancement of clinical technology in the area of medicine, dermatologists and other medical professionals now have access to a wide array of instruments that are related to medicine, allowing them to detect skin cancer more rapidly and lessen the disease's severity. Using cutting-edge CAD tools [3], malignant melanoma has been found and successfully diagnosed.

The meticulous introduction to the categorization of dermoscopy pictures is presented in this chapter for the reader's familiarization. In this chapter, we provided the platform for total skin lesion identification by utilizing dermoscopy pictures. This platform serves as an assistance to the CAD System, making it easier for physicians to evaluate lesions on patients. One last thing to mention is that the summary [4] should follow the arrangement of the thesis. Lesions may be caused by a broad variety of factors, including cysts, rashes, blisters, pus-filled sacs, discolorations, and swelling. Lesions can be solitary or numerous in number, and they can also spread extensively. Depending on

[1] *Nyemeesha V, Research Scholar, Department of CSE, Koneru Lakshmaiah Education Foundation,Vaddeswaram, AP, India nyemee@gmail.com

[2] M Kavitha, Associate Professor, Department of CSE, Koneru Lakshmaiah Education Foundation, Vaddeswaram, AP, India

mkavita@kluniversity.in

the depth of the scrape, the lesions might either be completely innocuous or a potentially fatal disease [5]. Finding strategies to reduce the amount of stress experienced by medical professionals is the focus of the current research being conducted in the area of medical diagnosis. This stress is caused by the classification of the lesions. There is a wide variety of skin diseases that are prevalent around the globe due to the widespread nature of the environment [6]. The following is a list of potential risk factors contribute to the growth of skin-related diseases: prolonged exposure to sunlight, viral infection, immunological suppression, and, moreover, hereditary abnormalities. Surgery is the only therapy that is recommended for early-stage melanoma [7], which is regarded to be the best technique for treating melanoma. A biopsy, broad excision, immunological check point inhibitors, and chemotherapy are some of the various potential treatments for melanoma that have been proposed throughout the course of time. It is believed that it is an iniquity to employ conventional ways in a scientifically sophisticated culture to minimize the relevance of cancer. This is because using traditional methods in such a society is considered to be an iniquity. Figure 1 displays some examples of the photos included in the ISIC-2019 dataset.

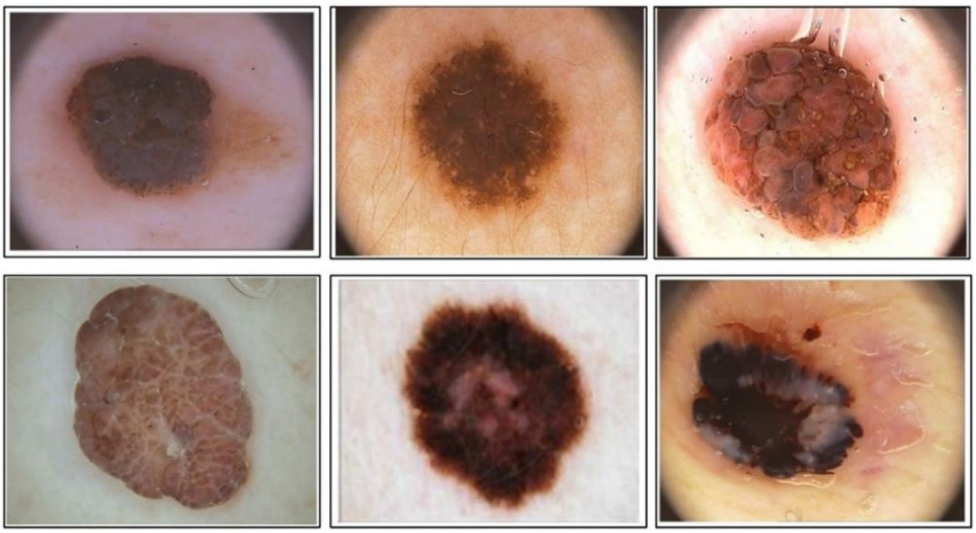

Figure 1. ISIC-2019 dataset sample images

The technological advancement connected to medical field will enable physicians and other medical professionals in properly treating a variety of medical-r skin cancers in a more expedient manner [8]. Unaided clinical exams used to be the predominant method for melanoma diagnosis throughout much of medical history. There has been a rising interest on the part of specialists in the use of visual examination for early identification of melanoma, despite the fact that there is both intra- and inter-variability among professionals. However, the conventional artificial intelligence methods were suffering with higher losses, which resulted in lower accuracy [9], and even after learning (training) it, analysis is still subjective. Despite this, artificial intelligence has improved diagnostic capabilities. Even though the diagnostic techniques that have been described for melanoma are fairly successful, using them might be challenging for both patients and pathologists. As a consequence of this, an increasing necessity for artificial intelligence based computerized automated diagnosis of skin lesion pictures that might provide promising avenues for CAD of melanoma. The most advanced CAD technologies [10] have been used in the process of finding and diagnosing malignant melanoma, which has resulted in the survival of hundreds of thousands of people diagnosed with the disease. The novel and unique contributions of this work as follows:

- Implementation of UG-Net for preprocessing and to achieve better hair removal and preprocessing performance.
- Implementation of HU-Net for segmentation operations for effectively localizing the disease effected region.
- Adoption of GLCM, DWT for extraction multiple features, i.e., colour, statistical and textures.
- Implementation of q-learning based DQNN model for classification of multiple skin cancer diseases.

- The simulations processed on real-time ISIC-2019 dataset proved that proposed SCDC-Net outperformed in superior subjective and qualitative performance as equated to existing process.

Remaining article is prepared as follows: section 2 involves analysis of various existing segmentation methods with their problem statement analysis. Section 3 gives operation details of proposed SCDC-Net with UG-Net preprocessing, HU-Net segmentation, feature extraction and DQNN classification. Section 4 involves about results analysis, i.e., subjective and objective performance estimation and performance comparison with existing methods. The essay is brought to a close in Section 5 with a conclusion and discussion of potential future scopes.

II. LITERATURE SURVEY

In this part, numerous methods for separating the lesion region from dermoscopic pictures that are found in various publications are thoroughly explored. Through the process of locating the clusters in conjunction with the neutrosophic c-means clustering (NCM), an efficient segmentation may be achieved. The authors of [11] describe histogram-based clustering estimation approach that can be used to effectively diagnose skin lesions. In order to categorize the pixels, you must first transform the dermoscopic visuals into characteristics based on the neutrosophic system [12]. The template is used to format your paper and style the text. All margins, column widths, line spaces, and text fonts are prescribed; please do not alter them. You may note peculiarities. For example, the head margin in this template measures proportionately more than is customary. This measurement and others are deliberate, using specifications that anticipate your paper as one part of the entire proceedings, and not as an independent document. Please do not revise any of the current designations. The HBCE algorithm makes use of the h-v and v-h approaches, respectively. The implementation is carried out with the assistance of the ISIC 2016 public data collection, which includes 900 photographs for training and 379 photos for testing purposes. The evaluation is performed by taking into consideration the ISIC 2016 data sets, which need efficient testing and training based on the availability of ground truth images. This allows for accurate results to be obtained from the evaluation. The results obtained from the work that was recommended are superior to those obtained using the traditional NCM technique that did not make use of HBCE. In [13], the authors presented an automatic lesion segmentation for the supplied dermoscopy images using a semi-supervised learning technique. This is done by using two steps: pre-processing and segmentation. The pre-processing step employs picture scaling using the bi-linear interpolation; the CLACHE algorithm improves the image's patchy lighting. The hair pixels are transformed using Frangivesselness filter and inpainting process with FMM [14]. Further, the pixels uniformity, such as color and texture properties, segmentation is used to separate the lesion patches. Grabcut method is applied to identify the approximate lesion for segmentation. This process is enhanced by applying k-means clustering, which groups pixels based on the RGB color conversion to forecast the precise lesion regions. Dice co-efficient values were increased utilizing deep learning methods to increase accuracy, and this is thought to be a future project.

The authors of [15] suggested a method known as the Quad-Tree melanoma detection system. This method is a precise expert color evaluation model that conducts color observation, and it is capable of quickly classifying lesions as either benign or malignant. The phrases concentric quartiles and Euclidean distance were covered in this article, both of which are applied in the process of analyzing melanomas. During the pre-processing step, the contrast between diseased background regions and foreground skin lesions is enhanced. This allows for a clearer differentiation between the two. Morphological procedures [16] such as top-hat and bottom-hat operations may be used to treat lesions that have a lower level of color contrast. The hybrid approach is applied for the effective identification of lesion boundaries; the procedure of segmentation is divided into two steps. The first step makes use of a modified Otsu threshold to identify core lesions, while the second stage makes use of an adaptive histogram function to extend the core lesion region along the radius. The enactment is assessed alongside a number of other classifiers, and the results lead to the conclusion that the classifier SVM gets the best performance with the features ROC curve.

Authors developed a unique meta-heuristic method called the DHOA-NN algorithm in reference to the work they did in [17]. The minute movements made by the buck are quickly detected, and the visual capacity of a buck is five times greater than that of a person, both of which contribute to the difficulty of the hunting process [18]. It might be difficult to keep track of the activities taking on at the higher level of the horizon. Therefore, it is said

that the hunters carry out their maneuvers in the relevant location. To do this with the use of an objective function, position update is performed for each iteration, until the best position is determined. Hence, it is concluded that that the convergence behavior of DHOA-NN is improved. The authors of [19] suggest using a segmentation recommender to cut down on the amount of time spent in training by relying on community sourcing and transfer learning. Both the ResNet50 [20] and the VGG16 were included into the system, and feature extraction was accomplished via their respective convolutional layers. The convolutional neural network (CNN) is a classifier that is made up of five nodes where each node represents a different segmentation technique, and based on this information an output layer is constructed. The two-dimensional structure of dermoscopy pictures allows for the recognition of the regional characteristics from a variety of different places. As a consequence of the investigation, it has been determined that the proposed method accurately predicts the segmentation methodology. The authors of [21] spoke about their examination of CNN design, which extends progressively and deeper into the convolution layers, in order to classify dermoscopic skin tumors using an inceptionv2 network. Within the context of the deep learning framework, an iterative procedure known as stochastic decent gradient is used for the purpose of training the inception v2 parameters [22]. The assessment procedure results in distinct sorts of outcomes from dermoscopic pictures, such as sonification and visual characteristics. The investigation came to the conclusion that the imaging approach known as tele-dermoscopy has improved accuracy and is a highly sensitive malignancy detector for both pigmented and non-pigmented lesions. This information was gathered from the sonification output.

Particle Swarm Optimization (PSO), a crucial component for skin cancer detection based on dermoscopy pictures, was used by the authors of reference [23]. In addition, different publications [24] have presented modified PSO algorithms for the purpose of feature analysis. These algorithms can choose the most useful characteristics. The initial population is split into two sub swarms, and the leader of each sub swarm guides the search for the optimal solution for the whole population by ensuring that fewer desirable options are eliminated. By employing the dynamic matrix representation [25] and probability distribution, a search with an extremely wide range of possibilities may be carried out. The proposed approach demonstrates significant improvement in the categorization of melanomas, and it also provides solutions to benchmark issues that are uni-modal and multi-modal. For the purpose of skin lesion segmentation, fully convolutional-deconvolutional networks (FCDN) were suggested by the authors of [26]. Here, the region of interest is calculated, so effected region is effectively identified. In [27] authors developed the deep learning adaptive networks for skin cancer classification, which contains the FCDN segmentation. However, this method has low computational complexity. Deep residual networks were created by the authors of [28] for the purpose of skin lesion categorization. These networks solve the disadvantages of adaptive networks.

In the article [29], the authors recommended comparing several picture segmentation approaches for analysis. The process of examining and detecting significant characteristics or objects exhibited within an image is referred to as segmentation [30]. The discontinuities of the edges are represented by edge-based segmentation, which is a crucial characteristic for image analysis and reflects the discontinuities in terms of intensity. By first computing a threshold value for a picture and then comparing it to the value of each pixel, the canny edge detector was used to get rid of broken edges in the image. The larger pixel value leads one to the conclusion that an edge must be there; otherwise, the possibility is eliminated. It is necessary to enclose the region that was chosen for the region-based segmentation [31]. Preprocessing is the first phase of the watershed transform. This step helps generate a well-segmented picture by lowering the amount of noise in the image and adjusting the intensity of it while still maintaining the information contained in the image. Therefore, it can be concluded that the edge detector canny offers the best performance when employing region expanding, which speeds up the process of segmentation [32] when contrasted with region splitting-and-merging.

The associated study that came after looked into several different feature extraction techniques. Only via effective feature extraction can accurate categorization be achieved. The characteristics of asymmetry, border, color, size, and edge were used in the process of classifying the various forms of cancer. Therefore, the recovered characteristics must be ABCDE in order to make sense. For instance, in the usual investigations [33], they extracted low-level, medium-level, and high-level features by using image processing. It is made by extracting several characteristics from the segmented lesion that are depending on the intensity and texture of the lesion. Techniques such as the discrete wavelet transform, local binary patterns, and grey level co-occurrence matrix-based feature extraction were used by the authors [34-35] in order to extract features from the data that they had

collected. The fact that the extracted features required to be modified in some way was the most significant disadvantage. The problems have been resolved by making use of feature selection techniques this time around. A wide range of possibilities, such as spectrum, color, shape, and textural alternatives, are used in order to choose the suitable characteristics for each particular feature. The chi-square test, the best-first search strategy, the gain ratio, the information gain, and the recursive feature removal procedures were all applied in the standard approaches [36]. By selecting just a few of features from the skin lesion graphs, one may get rid of the ABCDE attribute of the features. Transfer learning [37]-based algorithms are used in order to extract the appropriate properties for each skin lesion pixel that has been segmented. On the other hand, traditional transfer learning algorithms do not differentiate between variables that rely on illness and those that are peculiar to disease. This is because conventional transfer learning algorithms are not disease-specific. Therefore, the typical transfer learning algorithms have significant difficulties when dealing with skin cancer subtypes that are neither malignant nor melanoma. In the end, a literature review is conducted with an emphasis on machine learning tactics and transfer learning techniques. Support Vector Machines [38], Random Forests [39], and Navie Bayes [40] were some of the earliest categorization algorithms that saw widespread use in actual practice. These tactics performed well on very small datasets, but they were not successful on the datasets used in the ISIC competition. The classification of skin lesions has been accomplished with the assistance of artificial neural networks (ANN), namely Back-propagated ANN [41], DenseNet-201 [42], CNN with data augmentation (CNN-DG) [43], DLCNN [44], and MCM-CNN [45]. The authors of the study [46] found that using Ensemble hybrid CNN (HECNN) was effective in categorizing skin lesions into a wide variety of categories. In addition, the creation of DenseNet, SENet, and ResNeXt (DSR-Net) [47] has resulted in an improvement in the overall performance of machine learning models in comparison to prior models. In both the ISIC-2018 and ISIC-2019 competitions, this work took first and second prize, respectively.

III. PROPOSED METHOD

Artificial intelligence has improved diagnostic capabilities. Even though the diagnostic techniques that have been described for melanoma are fairly successful, using them might be challenging for both patients and pathologists. As a consequence of this, an increasing necessity for artificial intelligence based computerized automated diagnosis of skin lesion pictures that might provide promising avenues for CAD of melanoma. The most advanced CAD technologies have been used in the process of finding and diagnosing malignant melanoma, which has resulted in the survival of hundreds of thousands of people diagnosed with the disease. This work gives the analysis of suggested method for classification operation. Figure 2 is a block schematic of the SCDC-Net, and Table 1 is an algorithmic representation of the SCDC-Net

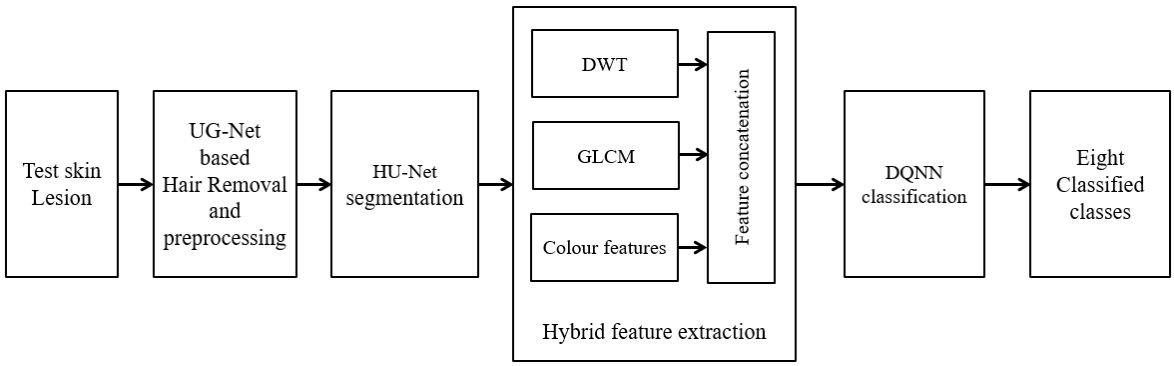

Figure 2. Proposed SCDC-Net Technique.

Table 1. Proposed SCDC-Net algorithm

Step 1: Train SCDC-Net system with ISIC-2019 dataset, which generates the multi-level trained features.

Step 2: Initially, UG-Net model adopted for preprocessing and hair removal operations. Here, U-Net model is used for hair segmentation, GAN model is used for hair gap inpainting. The detailed operations are described in section 3.1.

Step 3: Apply HU-Net for segmentation of skin cancer from UG-Net pre-processed outcome. Here, semantic segmentation with overlay approaches for efficient segmentation. The detailed operations are described in section 3.2.

Step 4: Further, multiple features extracted from HU-Net segmented outcome using GLCM, DWT, colour feature analysis. Here, low, statistical, texture, asymmetry, border, edge, colour, and diameter properties were extracted. The detailed operations are described in section 3.3.

Step 5: Train the DQNN model with features generated from step-4, which used for classification. The detailed operations are described in section 3.4.

Step 6: The test skin lesion image is applied to entire network, which resulted in identification of skin cancer type from available eight classes. The detailed operations are described in section 3.4.

Step 7: Estimate the performance of preprocessing, segmentation, feature extraction, classification models by calculating the confusion matrices. The detailed operations are described in section 4.

3.1 Hair removal and preprocessing using UG-Net

The hair and hair-like areas within skin lesion pictures must be removed and restored, to more effectively analyze features within lesions in order to differentiate between benign and malignant lesions and cancer. Further, the hair pixels, which are often present in dermoscopic pictures, obscure some of the lesion's details, including its border and texture. Therefore, these hair artifacts must be eliminated in melanoma identification and classification tasks. An automated hair removal technique that keeps all the lesion details while keeping the computational rate low enough to be employed is required in a real-time CAD tool. The literature hasn't thoroughly addressed the hair issue. Therefore, this section adopted the UG-Net model for preprocessing and hair removal operations. Here, U-Net model is used for hair segmentation, GAN model is used for hair gap inpainting. The suggested block design for the UG-Net model may be seen in Figure 3. Take a look at the photograph of the test lesion on your skin; it displays the hair area. The picture of the skin lesion is run through the U-Net model so that it may be segmented. Here, binary map of skin lesion is estimated. Then, GCN is used to analyse the area of hair pixels, which performs the hair gap inpainting operation to remove the hair free outcome image. This is a temporary skin lesion outcome called as coarse result. Then, the Intra-SSIM is calculated between coarse result to the original input skin lesion. Then, if intra-SSIM increases the UG-Net process is repeated, else intra-SSIM decreases improves the performance. Here, intra-SSIM cross-relation similarity, which acts as the bias vector. Finally, the pre-processed skin lesion is generated along with hair removal outcome.

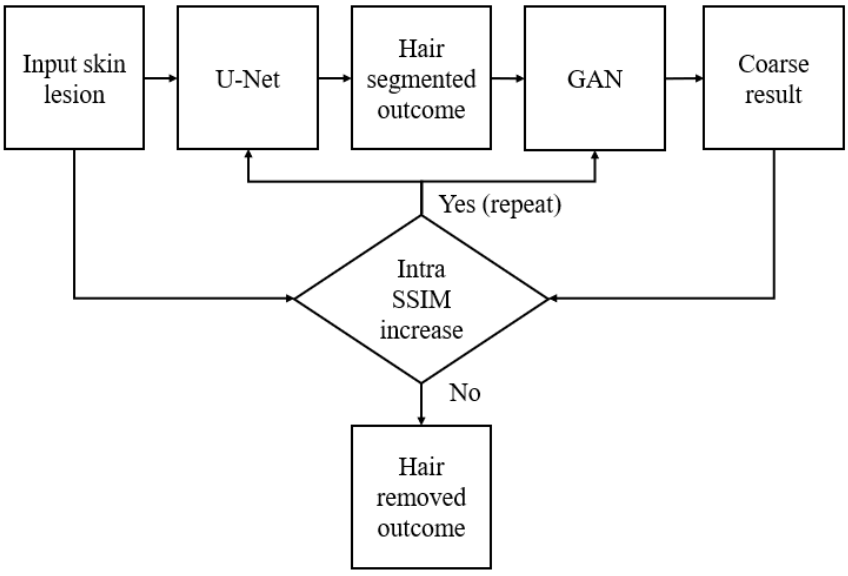

Figure 3. Operational diagram of UG-Net.

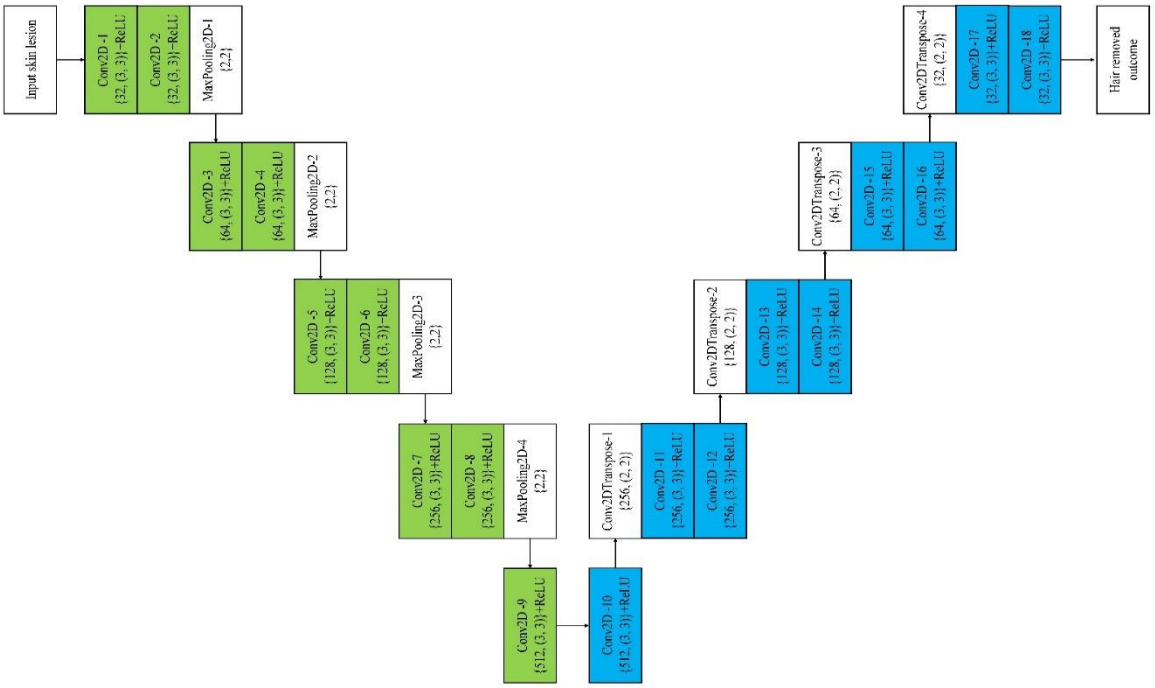

Figure 4. Layer-by-layer design of UG-Net.

Convolution layers, a batch normalization layer, rectified linear unit (ReLU) activation units, skip connections, max-pooling layers, and up-convolution layers are shown in Figure 4 as the many layers that make up the UG-Net's architecture. Here, convolution layers are used for feature extraction, batch normalization layer is adopted for synchronization, ReLU is used for selection of positive features, max-pooling is adopted for reduction (selection) of best features, and up-convolution are adopted for increase the number of features. Here, mainly the skip connections were established between down-sampling and up-sampling network, which maintains the synchronization between two sampling models. Finally, The SoftMax classifier is used in order to categorize the hair and non-hair pixels, which generates the hair removed binary map. In the architecture, {16,32,64,128} presented below the layer shows the number of kernels. Further, {(512 x 512), (256 x 256), …… (32 x 32)} presented left side of each layer shows that feature size (number of resultant features).

3.2 Segmentation using HU-Net

The challenge of segmenting skin lesions in a CAD system is made more difficult by changes in the form and size of the lesions. The first step in the CAD process is called "lesion segmentation," and it is used because it results in low error rates when assessing the structure, boundary, and size of a skin lesion. According to the inter-observer agreement of expert dermatologists, the skin lesion segmentation findings offered by current state-of-the-art deep learning segmentation algorithms do not deliver the essential results. This is because these approaches do not use the appropriate level of deep learning. Therefore, this section focused on development of HU-Net segmentation. The HU-Net functional diagram is seen in figure 5, below. Initially, UG-Net pre-processed outcome is applied to input of HU-Net. Then, semantic segmentation with overlay approaches for efficient segmentation by introducing the U-Net model. The U-Net model generates the binary ground truth map (binary mask) from pre-processed outcome. Further, pixel-wise multiplication operation is performed between pre-processed outcome to binary mask, which generates the final segmented outcome. Here, convolution layers are represented by blue colour, batch normalization layer are represented by white colour, skip connections are represented by gray colour arrow marks, and down-up samplings are represented by green colour arrow marks. Then, convolution layers, a batch normalization layer, ReLU activation units, skip connections, max-pooling layers, up-convolution layers, and up-convolution layers all contribute to HU-Net formation.

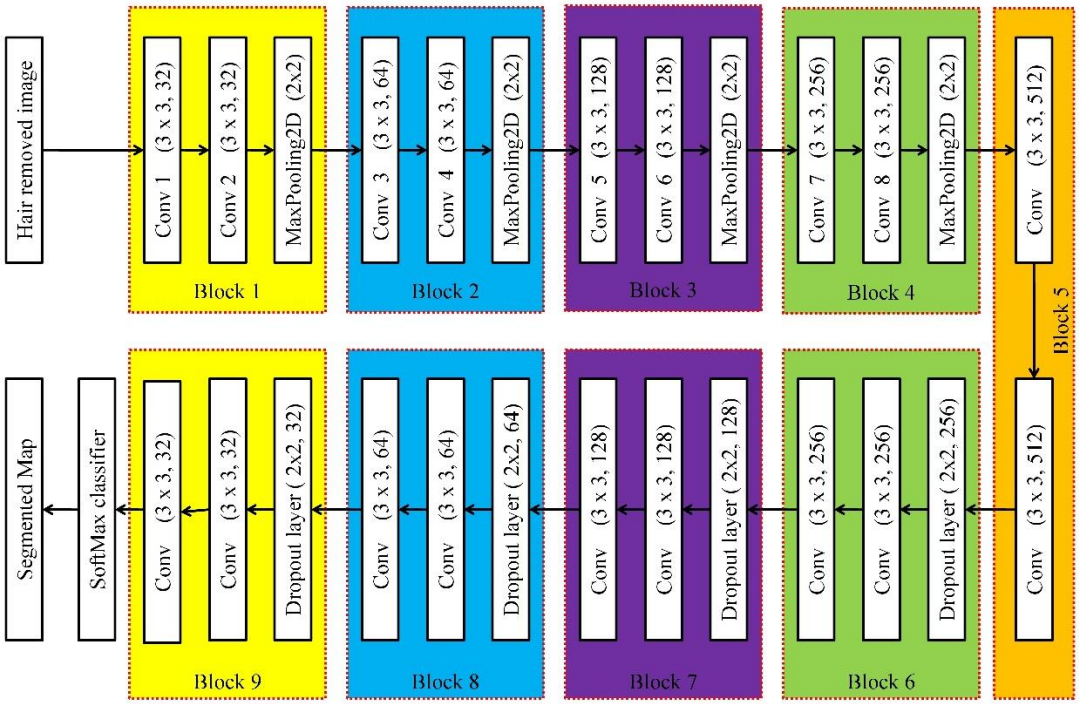

Figure 5. Layer wise architecture of HU-Net.

In this instance, convolution layers are utilized for the purpose of feature extraction, batch normalization layers are adopted for the purpose of synchronization, ReLU is utilized for the selection of positive features, max-pooling is adopted for the reduction (selection) of best features, and up-convolution are utilized for the purpose of increasing the number of features. In this case, the skip links between the down-sampling network and the up-sampling network were developed with the majority of their focus on being functional. These connections are responsible for keeping the synchronization between the two sampling models. In the end, the SoftMax classifier is used to differentiate between pixels affected by the disease and those that are unaffected by it, which results in the generation of a binary segmented map. In the architecture, {64,128, …,1024} presented top of the layer shows the number of kernels. Further, {(224 x 384), …… (14 x 24)} presented left side of each layer shows that feature size (number of resultant features).

3.3. Multi-level feature extraction

The HU-Net segmented outcome is applied as input to multi-level feature extraction process. Here, GLCM feature extraction is used to extract low, statistical, texture, asymmetry, border, edge, colour, and diameter properties. The term "directionality of picture texture" refers to the statistic of pixel changes within an area that shows the similarity and regularity of the pixel gray value in different directions. This indicates that the statistic of the change in pixel gray in a number of different directions may be able to express the directionality of texture images. Texture is a trait that refers to the integration of structural qualities on a large scale and statistical characteristics on a small scale. Consequently, the direction measure must, to some degree, represent the structure of the picture data, but it may also reflect the statistical features of the image pixels. This is because of the way that the direction measure works. In order to describe the texture characteristic, the direction measure statistic was developed for the purpose of this research. It can determine the high-order statistical feature of texture and is based on the directionality of the image. A high rate of identification may be achieved using the high-order direction measure when applied to realistic textures. Using the direction measure, the picture is segmented into many directions, and the change in the gray value of the image in each direction is analyzed. A quantifiable answer for the rate at which the picture pixels change in each direction is produced as a consequence of this process. According to the following definition, direction measure refers to the amount of change that occurs in the pixel values of the surrounding area in each

direction: Assume that the picture is N pixels wide and M pixels tall, and that the coordinates p and q may refer to any point in the image. Arrange the image's pixels in row-major order, with (p, q) being equivalent to point j (j = 1, 2, 3..., N x M), assuming that j = 1, 2, 3,.. N x M. Figure 6 then illustrates the 4x4 neighborhood window of the direction measure that is centered on (p, q). Here, "d(k)|k = 1, 3, 5, 7" signifies the four direction measures that are, and the value of "d(k)" is a measure of the texture change in this direction. Figure 6 also depicts the neighborhood window of the direction measure that is centered on (p, q).

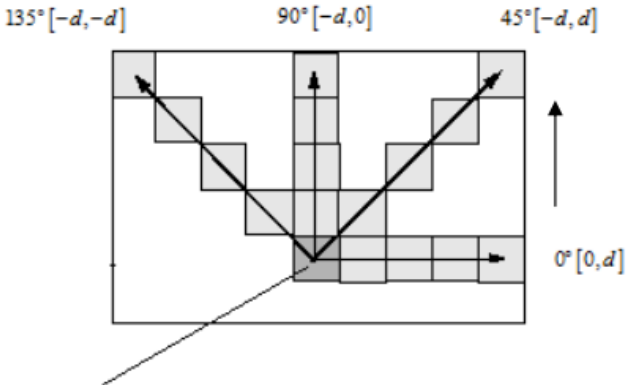

Figure 6. GLCM feature extraction process

Further, the following equations (1) to (5) shows the extracted features such as contrast, homogeneity, correlation, Angular Second Moment (ASM), and energy properties. The DWT features also extracted parallelly from HU-Net segmented outcome. Figure 7 shows the extracted features using DWT process. Here, low-low (LL1, LL2), low-high (LH1, LH2), high-low (HL1, HL2), and high-high (HH1, HH2) features are extracted. Moreover, these features were extracted by applying the low pass filter, high pass filter combinations on rows, columns of HU-Net segmented outcome. Further, only LL2 features are contain high-seismic data.

$$\text{Contrast} = \sum_{a,b=0}^{N-1} S_{a,b}\,(a-b)^2 \tag{1}$$

$$\text{Homogeneity} = \sum_{a,b=0}^{N-1} \frac{S_{a,b}}{1+(a-b)^2} \tag{2}$$

$$\text{Correlation} = \sum_{a,b=0}^{N-1} S_{a,b}\left[\frac{(a-\mu_a)(b-\mu_b)}{\sqrt{(\sigma_a^2)(\sigma_b^2)}}\right] \tag{3}$$

$$\text{ASM} = \sum_{a,b=0}^{N-1} s_{a,b}^2 \tag{4}$$

$$\text{Energy} = \sqrt{ASM} \tag{5}$$

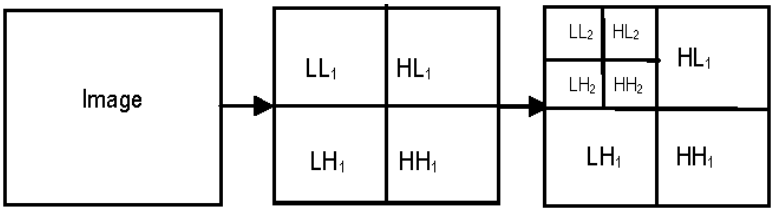

Figure 7. Feature extraction using DWT.

The color features generated in following passion, where Mean (μ), standard deviation (σ) metrics were estimated from segmented outcome.

$$\mu = \frac{1}{N^2}\sum_{i,j=1}^{N} I(i,j) \quad (6)$$

$$\sigma = \sqrt{\frac{\sum_{i,j=1}^{N}[I(i,j)-\mu]^2}{N^2}} \quad (7)$$

After that, each of these functions is brought together with the array concatenation technique, producing a hybrid multi-level feature matrix as the output.

3.4 Classification

The Q-Learning approach is required as a requirement since it generates an accurate matrix for the working agent, which the agent may "refer to" in order to maximize the amount of compensation it receives during the course of its employment. This strategy is not intrinsically flawed; nonetheless, it is applicable in only the most constrained of settings, and it quickly loses its viability as the number of states and activities in the environment increases. The revelation that the values in the matrix only have relative significance—that is, importance only with relation to the other values—provides the solution to the challenge that was described earlier in the sentence. As a result of this, we have arrived at the DQNN algorithm, which makes use of a deep neural network to approximate the calculation of the values. This close proximity of values does not constitute a problem as long as the relative importance is preserved. It is necessary to provide the neural network with the beginning state for it to be able to operate properly. The neural network will then provide the Q-value for each possible action that might be done. In contrast to the purpose of other popular Deep Learning procedures, which remains the same throughout, the target for the neural network in this approach changes throughout. This problem may be handled by using two neural networks in instead of a single one. The parameters of a second neural network are computed by a first network that has the same architecture as the first network but uses a different set of parameters. The first network is used to adjust the parameters of the network. After a certain number of repetitions in the parent network, the parameters are then duplicated to the target network. Figure 8 depicts the layer-by-layer architecture of DQNN, which is used in the classification of various illness classifications based on test skin images. The Q-properties of test samples are compared with pre-trained samples, which results the classification outcome.

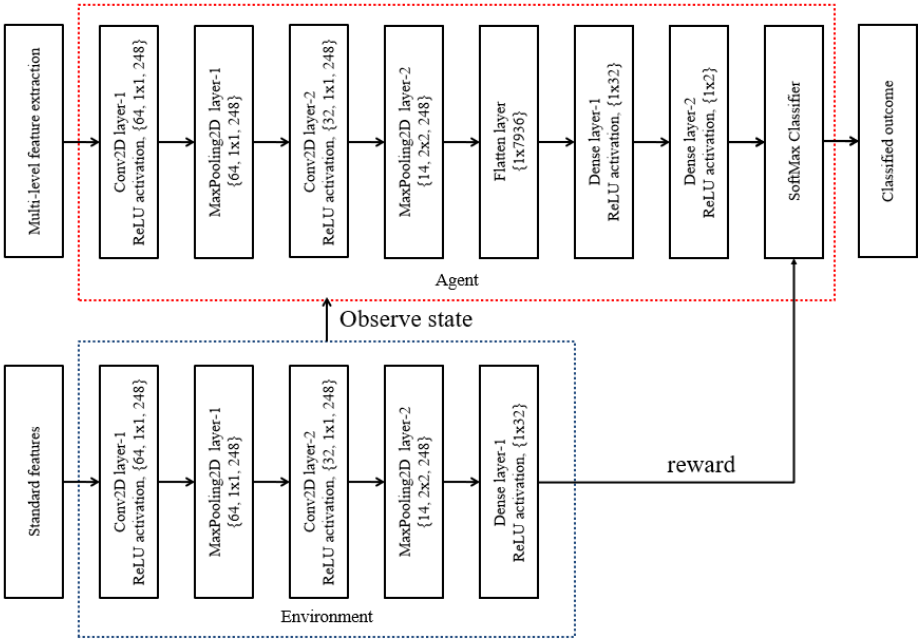

Figure 8. Layer wise architecture of DQNN.

IV.EXPERIMENTATION ENVIRONMENT

This section involves about results analysis, i.e., subjective and objective performance estimation and performance comparison with existing methods. Further, the proposed SHRS-Net is implemented using MatlabR2020a environment with deep learning libraries. The performance of proposed and existing methods is verified under same environment with same dataset.

4.1 *Dataset*

The suggested method was trained with the use of the ISIC 2019challenge dataset, which is available to the general public. This dataset incorporates the HAM10000 and the BCN 20000 sub datasets among its constituents. The HAM10000 dataset has 10000 different lesions, each of which is composed of 600450 individual pixels. On BCN 20000, there are a total of 19424 lesions, and the size of each one is 1024 by 1024. The ISIC dataset includes a total of 25,331 skin lesions, which are separated into the following categories: There are 628 skin lesions caused by SCC, 239 caused by DF, 867 caused by AKIEC, 2624 caused by BKL, 3,323 caused by BCC, and 4,522 caused by MEL. The information is presented in three distinct parts. The dataset utilized for testing is 10%, the dataset used for validation is 10%, and the dataset used for training is 80%.

4.2 *Subjective evaluation*

Figure 9 contains three samples of images, which shows the effectiveness of UG-Net method hair removal performance. Figure 9(a) represents test skin lesion image, figure 9(b) represents the disease effected region, figure 9(c) represents the hair region, figure 9(d) shows the outcomes effected region. Figure 6 shows the proposed SHRS-Net segmentation performance.

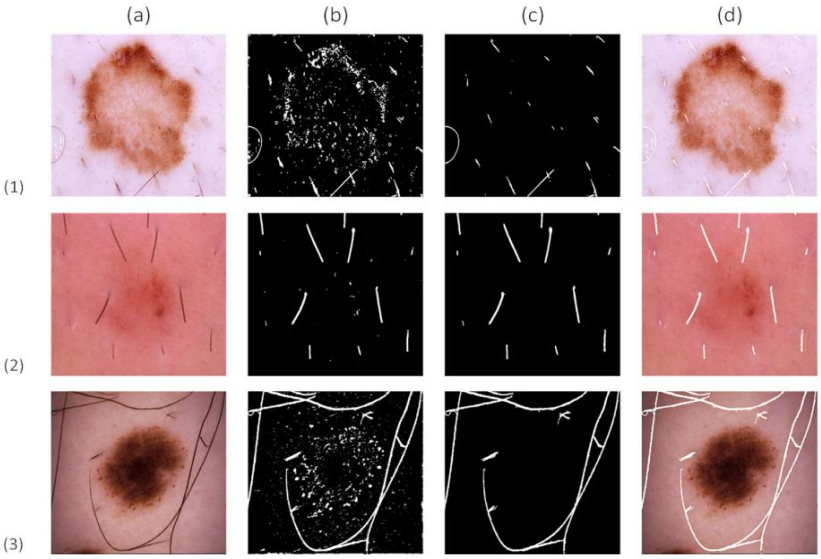

Figure 9. UG-Net hair removal outcomes.

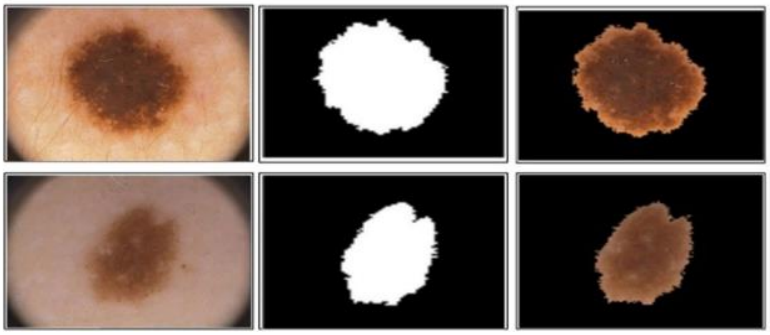

Figure 10. Segmentation outcomes using HU-Net.

Figure 10 shows the segmented outcomes using UG-Net. The source input skin lesion photos are located in the first column of this table, while the ground truth skin lesion images, complete with disease area and hair region, are located in the second column, third column contains the proposed hair removed output images, and fourth column contains the proposed segmented output images.

4.3 *Objective evaluation*

4.3.1 *Preprocessing methods performance estimation*

Nine qualitative objective indicators are included in this article for assessing hair removal analysis. In the second category, you'll find measurements such as the UQI and MS-SSIM, both of which represent statistical characteristics of the area. VIF and PSNR data were employed so that the results of the simulation could be compared to those of the PSNR-HVS. In this instance, hair removal increased the quality of the repaired lesion, which is why the system recorded the greatest result. The suggested UG-Net on the nine criteria is compared to that of different industry standards in Table 2. The MSE and RMSE of the suggested technique are negligible, demonstrating the accuracy of the rebuilt lesion. This indicates that the SSIM and MSSSIM of the recreated lesion are quite close to those of the original skin lesion.

Metric	**UG-Net**	ADF [17]	BHF [16]	FGF CEF [15]	TL-CNN [18]	HI [14]	CUOI [13]	CTI [12]
SSIM	0.998	0.867	0.885	0.851	0.926	0.890	0.864	0.921
MSE	0.998	258.347	103.903	404.366	27.47	175.303	221.346	55.311
RMSE	0.512	14.226	9.207	15.485	4.790	11.032	13.287	6.318
PSNR	49.138	26.080	29.87	27.001	35.17	29.158	26.570	33.096
UQI	0.99999	0.991	0.996	0.990	0.997	0.995	0.992	0.997
VIF	0.917	0.526	0.499	0.402	0.525	0.531	0.509	0.592
PSNR-HVS-M	55.945	25.078	29.404	26.248	36.802	28.445	25.519	33.005
MSSSIM	0.99999	0.870	0.934	0.917	0.998	0.945	0.875	0.955
PSNR-HVS	52.248	24.628	28.681	25.738	35.168	27.826	25.065	32.186

Table 2. Preprocessing methods performance estimation

4.3.2 Segmentation analysis

The segmentation effectiveness of HU-Net is determined using six objective criteria. The method precisely separates the skin lesion and records the greatest results. Table 3 compares the segmentation presentation estimation and comparison with existing approaches. The literature provides documentation of these techniques' drawbacks. a published, non-participant study using algorithms to segment skin cancer. Since the skin lesions were first cleared of noise and hair, in comparison to the several alternative methods, the HU-Net segmentation that was recommended had the most successful outcomes. The percentage of successfully segmented pixels is represented by the SSEN parameter. In this manner, the HU-Net segmentation efficiently separates the skin lesion pixels. Pixels that represented non-skin lesions were correctly recognized but were not segmented since the HU-Net technique provides the maximum degree of specificity. Using the HU-Net approach, the proper segments of the cutaneous lesion have been created. The HU-Net method in this investigation had the highest SSPE, properly segmenting the skin lesions. The SSEN between segmented output and the original lesions was highest when using the HU-Net method. The suggested method further enhances performance by identifying specific properties for each pixel and optimizing the training loss.

Method	**CDNN [26]**	**FCRN [27]**	**AlexaNet [28]**	**PSPNet [30]**	**JAM-NET [31]**	**U-Net [32]**	**HU-Net**
SSEN	82.5	82	80.2	85.34	90.38	93.86	99.999
SSPE	97.5	97.8	98.5	98.88	99.23	99.4	99.989
SDIC	84.9	84.7	84.4	86.73	90.46	93.23	99.979

SJAC	76.5	76.2	76	78.83	82.48	86.35	99.909
SACC	93.4	93.2	93.4	95.23	96.37	96.45	99.913
SMCC	95.39	95.2	96.93	96.29	97.38	97.45	99.9948

Table 3. Segmentation methods performance estimation

4.3.3 Feature extraction analysis

Table 4 compared the performance of various feature extraction methods. Here, proposed DWT-GLCM resulted in superior performance compared to other methods like LFN-CNN [27], and RNN [23] for all metrics. Here, FSEN, FACC, FPRE, FSPE, and FAUC metrics were measured to prove the robust process of proposed method.

Method	FSEN	FACC	FPRE	FSPE	FAUC
LFN-CNN [27]	66.56	91.4	40.9	91.5	0.833
RNN [23]	34.2	92	64.1	88.1	0.795
Proposed Color-DWT-GLCM	98.89	99.99	99.19	99.09	0.9781

Table 4. Feature extraction methods performance estimation.

4.3.4 Classification Analysis

Table 5 compared the performance of various classification methods. Here, proposed SCDC-Net resulted in better categorization performance than other approaches like MCM-CNN [45], CNN-DG [43], DenseNet 201[42], and CNN [44] for all metrics. Here, CSEN, CACC, CPRE, CSPE, and CAUC metrics were measured to prove the robust process of proposed method. The receiver operating characteristic (ROC) curve can be shown in Figure 11, and it can be seen that the proposed SCDC-Net attained a value of 0.96 for its ROC.

Method	CSEN	CACC	CPRE	CSPE	CAUC
MCM-CNN [45]	93.24	95.39	92.28	94.58	0.902
CNN-DG [43]	66.2	66.2	78	95.2	0.915
DenseNet 201[42]	82.4	85.8	84.67	89.35	0.893
CNN [44]	74	81	77	84	0.834
Proposed SCDC-Net	**99.78**	**99.987**	**99.92**	**99.78**	**0.9978**

Table 5. Classification methods performance estimation.

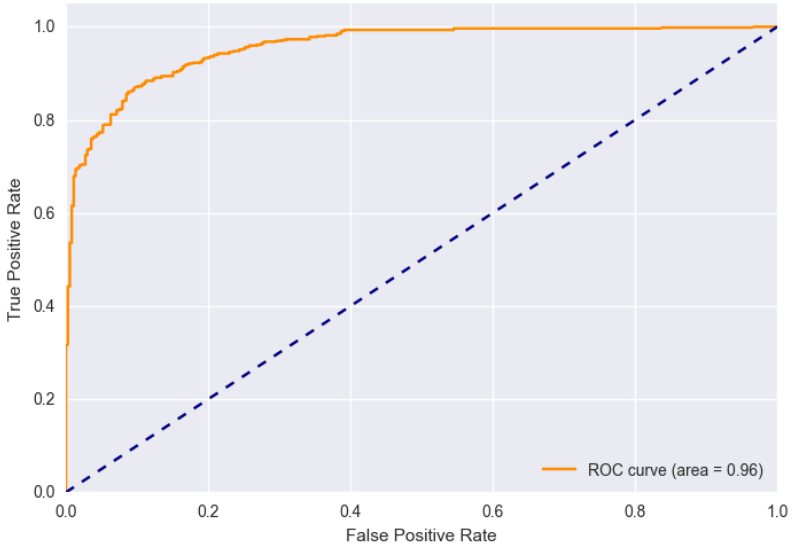

Figure 11. ROC Curve of SCDC-Net

V.CONCLUSION

The increase in radiation in the atmosphere is to blame for the global spread of the skin cancer condition. One of the worst illnesses, skin cancer claims millions of lives each year all over the world. Therefore, early skin cancer diagnosis with CAD technology may save lives. Hair artifacts and poor lesion segmentation, however, have an impact on how skin cancer is classified. Due to poor feature analysis, traditional approaches were unable to provide greater performance. As a result, the transfer learning-based SCDC-Net was built for this study to accomplish the robust presentation. Initially, for the purpose of removing hair from skin lesions and so enhancing the area of interest, the UG-Net model, which is generated by fusing the U-Net and GAN models, was proposed. Additionally, HU-Net does the segmentation operation to pinpoint the area of interest that is affected by the illness. Additionally, the GLCM matrix and DWT are used to extract the features, which extracts the statistical, color, and texture characteristics. Finally, a DQNN model that can classify different kinds of skin cancer illness is trained using these integrated characteristics. The simulations performed on the live ISIC-2019 dataset demonstrated that the proposed SCDC-Net beat current approaches in every performance metric. The major advantage of this work is that improved segmentation, classification performance. This study may be expanded with more sophisticated models for categorizing diseases within itself. So, channel and spatial attention methods will be adopted to extract the more intra -disease features. Further, graph neural networks can be also included to improve the overall performance of system.

REFERENCES

[1] Varma, P. Bharat Siva, et al. "SLDCNet: Skin lesion detection and classification using full resolution convolutional network-based deep learning CNN with transfer learning." *Expert Systems*: e12944.

[2] Iqbal, Junaid. "Dermatologist-level classification of skin cancer with deep neural networks." (2021).

[3] Abdar, Moloud, et al. "Uncertainty quantification in skin cancer classification using three-way decision-based Bayesian deep learning." *Computers in biology and medicine* 135 (2021): 104418..

[4] Bratchenko, Ivan A., et al. "Classification of skin cancer using convolutional neural networks analysis of Raman spectra." *Computer Methods and Programs in Biomedicine* 219 (2022): 106755.

[5] Maniraj, S. P., and P. Sardar Maran. "A hybrid deep learning approach for skin cancer diagnosis using subband fusion of 3D wavelets." *The Journal of Supercomputing* (2022): 1-16.

[6] Thomas, Simon M., et al. "Interpretable deep learning systems for multi-class segmentation and classification of non-melanoma skin cancer." *Medical Image Analysis* 68 (2021): 101915.

[7] Pacheco, Andre GC, and Renato A. Krohling. "An attention-based mechanism to combine images and metadata in deep learning models applied to skin cancer classification." *IEEE journal of biomedical and health informatics* 25.9 (2021): 3554-3563.

[8] Jagadesh, B. N., K. Srinivasa Rao, and Ch Satyanarayana. "A unified approach for skin colour segmentation using generic bivariate Pearson mixture model." *International Journal of Advanced intelligence paradigms* 15.1 (2020): 17-31.

[9] Abbas, Alaa Ahmed, and Fadeheela Sabri Abu-Almash. "Skin lesion border detection based on optimal statistical model using optimized colour channel." Journal of Autonomous Intelligence 3.1 (2020): 18-26.

[10] Hemalatha, R. J., et al. "A comparison of filtering and enhancement methods in malignant melanoma images." *2017 IEEE International Conference on Power, Control, Signals and Instrumentation Engineering (ICPCSI)*. IEEE, 2017.

[11] Sharma, Varun, Ananth Garg, and S. Thenmalar. A survey on Classification of malignant melanoma and Benign Skin Lesion by Using Machine Learning Techniques. No. 2611. EasyChair, 2020.

[12] . T. B. Toossi, H. R. Pourreza, H. Zare, M.-H. Sigari, P. Layegh, and A. Azimi, ‘‘An effective hair removal algorithm for dermoscopy images,’’ Skin Res. Technol., vol. 19, no. 3, pp. 230–235, Aug. 2013.

[13] P. Bibiloni, M. González-Hidalgo, and S. Massanet, ‘‘Skin hair removal in dermoscopic images using soft color morphology,’’ in Proc. Conf. Artif. Intell. Med. Eur. Cham, Switzerland: Springer, 2017, pp. 322–326.

[14] Salido, Julie Ann A., and Conrado Ruiz Jr. "Using morphological operators and inpainting for hair removal in dermoscopic images." *Proceedings of the Computer Graphics International Conference*. 2017.

[15] Kang, Dongwann, Sansggeun Kim, and Sangoh Park. "Flow-guided hair removal for automated skin lesion identification." *Multimedia Tools and Applications* 77.8 (2018): 9897-9908.

[16] H Khan, Adil, et al. "Classification of skin lesion with hair and artifacts removal using black-hat morphology and total variation." *International Journal of Computing and Digital Systems* 10 (2020): 2-8.

[17] Sau, Kartik, AnanjanMaiti, and Anay Ghosh. "Preprocessing of skin cancer using anisotropic diffusion and sigmoid function." *Advanced Computational and Communication Paradigms*. Springer, Singapore, 2018. 51-61.

[18] Talavera-Martínez L, Bibiloni P, González-Hidalgo M. Hair Segmentation and Removal in Dermoscopic Images using Deep Learning. IEEE Access. 2020 Dec 24.

[19] Rahmat, RomiFadillah, et al. "Skin color segmentation using multi-color space threshold." *2016 3rd International Conference on Computer and Information Sciences (ICCOINS)*. IEEE, 2016.

[20] Zortea, Maciel, Eliezer Flores, and Jacob Scharcanski. "A simple weighted thresholding method for the segmentation of pigmented skin lesions in macroscopic images." *Pattern Recognition* 64 (2017): 92-104.

[21] Xie, H., Zhang, L., Lim, C. P., Yu, Y., Liu, C., Liu, H., & Walters, J. (2019). Improving K-means clustering with enhanced firefly algorithms. *Applied Soft Computing*, *84*, 105763.

[22] Nida, Nudrat, et al. "Melanoma lesion detection and segmentation using deep region based convolutional neural network and fuzzy C-means clustering." *International journal of medical informatics* 124 (2019): 37-48.

[23] Soomro, Shafiullah, Asad Munir, and Kwang Nam Choi. "Fuzzy c-means clustering based active contour model driven by edge scaled region information." *Expert Systems with Applications* 120 (2019): 387-396.

[24] Hawas, Ahmed Refaat, et al. "OCE-NGC: A neutrosophic graph cut algorithm using optimized clustering estimation algorithm for dermoscopic skin lesion segmentation." *Applied Soft Computing* 86 (2020): 105931.

[25] Tan, Teck Yan, Li Zhang, and Chee Peng Lim. "Adaptive melanoma diagnosis using evolving clustering, ensemble and deep neural networks." *Knowledge-Based Systems* 187 (2020): 104807.

[26] Y. Yuan, M. Chao and Y.-C. Lo, "Automatic skin lesion segmentation with fully convolutional-deconvolutional networks," arXiv: 1703.05165, 2017

[27] Li, Yuexiang, and Linlin Shen. "Skin Lesion Analysis Towards Melanoma Detection Using Deep Learning Network." *arXiv preprint arXiv:1703.00577* (2017).

[28] L. Bi, K. Jinman, E. Ahn and D. Feng, "Automatic skin lesion analysis using large-scale dermoscopy images and deep residual networks," in arXiv: 1703.04197, 2017.

[29] Design and implementation of student chat bot using AIML and LSA Naga Lakshmi, K., Kishore Reddy, Y., Kireeti, M., Swathi, T., Ismail, M.2019International Journal of Innovative Technology and Exploring Engineering 8(6), pp. 1742-1746

[30] Zou, J., Ma, X., Zhong, C., Zhang, Y.: Dermoscopic image analysis for ISIC challenge (2018). arXivPrepr arXiv:180708948

[31] Hardie, Russell C., et al. "Skin lesion segmentation and classification for ISIC 2018 using traditional classifiers with hand-crafted features." *arXiv preprint arXiv:1807.07001* (2018).

[32] Abraham, Nabila, and NaimulMefraz Khan. "A novel focal tversky loss function with improved attention u-net for lesion segmentation." *2019 IEEE 16th International Symposium on Biomedical Imaging (ISBI 2019)*. IEEE, 2019.

[33] Chatterjee, Saptarshi, et al. "Extraction of features from cross correlation in space and frequency domains for classification of skin lesions." *Biomedical Signal Processing and Control* 53 (2019): 101581.

[34] Improved fractal image compression using range block size Ismail, B.M., Basha, S.M., Reddy, B.E.20162015 IEEE International Conference on Computer Graphics, Vision and Information Security, CGVIS 2015 pp. 284-289

[35] Alfed, Naser, and Fouad Khelifi. "Bagged textural and color features for melanoma skin cancer detection in dermoscopic and standard images." *Expert Systems with Applications* 90 (2017): 101-110.

[36] Tan, Teck Yan, et al. "Intelligent skin cancer detection using enhanced particle swarm optimization." *Knowledge-based systems* 158 (2018): 118-135.

[37] Amin, Javeria, et al. "Integrated design of deep features fusion for localization and classification of skin cancer." *Pattern Recognition Letters* 131 (2020): 63-70.

[38] Bakay, MelahatSevgül, and ÜmitAğbulut. "Electricity production based forecasting of greenhouse gas emissions in Turkey with deep learning, support vector machine and artificial neural network algorithms." *Journal of Cleaner Production* 285 (2021): 125324.

[39] Li, Xiaohui, et al. "Discrimination of soft tissues using laser-induced breakdown spectroscopy in combination with k nearest neighbors (kNN) and support vector machine (SVM) classifiers." *Optics & Laser Technology* 102 (2018): 233-239.

[40] Balaji, V. R., et al. "Skin disease detection and segmentation using dynamic graph cut algorithm and classification through Naive Bayes classifier." *Measurement* 163 (2020): 107922.

[41] Hekler, Achim, et al. "Superior skin cancer classification by the combination of human and artificial intelligence." *European Journal of Cancer* 120 (2019): 114-121.

[42] Guissous, AllaEddine. "Skin lesion classification using deep neural network." *arXiv preprint arXiv:1911.07817* (2019).

[43] Nyemeesha, V., Ismail, B.M. Implementation of noise and hair removals from dermoscopy images using hybrid Gaussian filter Network Modeling Analysis in Health Informatics and Bioinformatics Volume 10, Issue 1, December 2021

[44] [Kassem, Mohamed A., Khalid M. Hosny, and Mohamed M. Fouad. "Skin lesions classification into eight classes for ISIC 2019 using deep convolutional neural network and transfer learning." *IEEE Access* 8 (2020): 114822-114832.

[45] High rate compression based on luminance & chrominance of the image using Binary Plane Technique Mohammed Ismail, B., Shaik, M.B., Eswara Reddy, B.2012Journal of Theoretical and Applied Information Technology 42(2), pp. 191-195

[46] Nozdryn-Plotnicki, A., Yap, J., &Yolland, W. (2018). Ensembling convolutional neural networks for skin cancer classification. International Skin Imaging Collaboration (ISIC) Challenge on Skin Image Analysis for Melanoma Detection. MICCAI.

[47] Nyemeesha V., Ismail B.M. (2021) Method to Enhance Classification of Skin Cancer Using Back Propagated Artificial Neural Network Applied Intelligence and Informatics. AII 2021. Communications in Computer and Information Science, vol 1435. Springer, Cham. https://doi.org/10.1007/978-3-030-82269-9_9

[48] Pacheco, Andre GC, Abder-Rahman Ali, and Thomas Trappenberg. "Skin cancer detection based on deep learning and entropy to detect outlier samples." *arXiv preprint arXiv:1909.04525* (2019).

[49] Marc Combalia, Noel C. F. Codella, Veronica Rotemberg, Brian Helba, Veronica Vilaplana, Ofer Reiter, Allan C. Halpern, Susana Puig, JosepMalvehy: “BCN20000: Dermoscopic Lesions in the Wild”, 2019; arXiv:1908.02288.